JOC Article

Self-Assembled Fluorescent Hexaazatriphenylenes That Act as a Light-Harvesting Antenna

Tsutomu Ishi-i,*,†,‡ Koh-ichi Murakami,§ Yusuke Imai,|| and Shuntaro Mataka*,†

Institute for Materials Chemistry and Engineering (IMCE), Kyushu University, 6-1 Kasuga-koh-en, Kasuga 816-8580, Japan, Department of Biochemistry and Applied Chemistry, Kurume National College of Technology, 1-1-1 Komorino, Kurume 830-8555, Japan, Interdisciplinary Graduate School of Engineering Sciences, Kyushu University, 6-1 Kasuga-koh-en, Kasuga 816-8580, Japan, and On-site Sensing and Diagnosis Research Laboratory, National Institute of Advanced Industrial Science and Technology (AIST), 807-1 Shuku-machi, Tosu, Saga 841-0052, Japan

ishi-i@kurume-nct.ac.jp

Received April 12, 2006

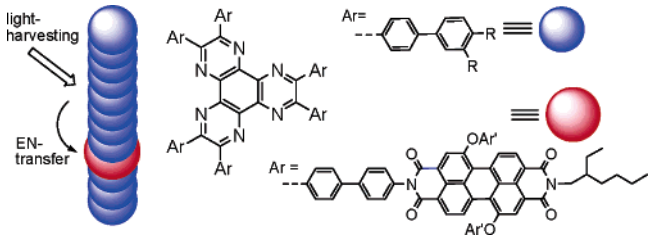

In this paper we report the self-assembling nature of fluorescent hexaazatriphenylenes (HATs) **6a**−**d** with six alkyl/alkoxy-chain-containing biphenyl groups and their application to light-harvesting antennae. In a nonpolar solvent and the film state, the HAT derivatives form one-dimensional aggregates with an H-type parallel stacking mode, which were analyzed by ^{1}H NMR, UV−vis, and steady-state and time-resolved fluorescence spectroscopy. When HAT derivative **7** with six perylenediimide moieties is incorporated into the one-dimensional aggregates, an efficient energy transfer takes place from the self-assembled HAT moiety as a light-harvesting antenna to the perylenediimide moiety as an energy acceptor. Further, when HAT derivative **8** with six triphenylamino moieties is newly added to the light-harvesting system, an intermolecular electron transfer occurs subsequently between the electron-accepting perylenediimide molecule and the electron-donating triphenylamino molecule.

Introduction

Energy and electron transfer in a donor−acceptor system has been of much interest in recent years because it is an important process in a natural photosynthetic system[1] as well as artificial photovoltaic.[2] In the natural system, antenna chlorophyll moieties are self-assembled in a highly ordered manner to achieve light harvesting and energy transfer with extremely high efficiency.[3] The noncovalent synthesis used in the natural system has been widely developed as a novel strategy to construct artificial antenna moieties such as self-assembled multiporphyrin systems.[4−7] Recently, long-range ordering in well-defined

* To whom correspondence should be addressed. Phone: +81-942-35-9404. Fax: +81-942-35-9400.
† IMCE, Kyushu University.
‡ Kurume National College of Technology.
§ Interdisciplinary Graduate School of Engineering Sciences, Kyushu University.
|| AIST.

(1) Deisenhofer, J.; Michel, H. *Angew. Chem., Int. Ed. Engl.* **1989**, *28*, 829−847.
(2) (a) Gust, D.; Moore, T. A.; Moore, A. L. *Acc. Chem. Res.* **2001**, *34*, 40−48. (b) Choi, M.-S.; Yamazaki, T.; Yamazaki, I.; Aida, T. *Angew. Chem., Int. Ed.* **2004**, *43*, 150−158. (c) Imahori, H. *J. Chem. Phys. B* **2004**, *108*, 6130−6143.
(3) (a) Kühlbrandt, W.; Wang, D. N.; Fujiyoshi, Y. *Nature* **1994**, *367*, 614−621. (b) McDermott, G.; Prince, S. M.; Freer, A. A.; Hawthornthwaite-Lawless, A. M.; Papiz, M. Z.; Cogdell, R. J.; Isaacs, N. W. *Nature* **1995**, *374*, 517−521. (c) Karrasch, S.; Bullough, P. A.; Ghosh, R. *EMBO J.* **1995**, *14*, 631−638. (d) Koepke, J.; Hu, X.; Muenke, C.; Schulten, K.; Michel, H. *Structure* **1996**, *4*, 581−597. (e) McLuskey, K.; Prince, S. M.; Cogdell, R. J.; Isaacs, N. W. *Biochemistry* **2001**, *40*, 8783−8789. (f) Roszak, A. W.; Howard, T. D.; Southall, J.; Gardiner, A. T.; Law, C. J.; Isaacs, N. W.; Cogdell, R. J. *Science* **2003**, *302*, 1969−1972.
(4) (a) Ogawa, K.; Kobuke, Y. *Angew. Chem., Int. Ed.* **2000**, *39*, 4070−4073. (b) Takahashi, R.; Kobuke, Y. *J. Am. Chem. Soc.* **2003**, *125*, 2372−2373. (c) Ikeda, C.; Satake, A.; Kobuke, Y. *Org. Lett.* **2003**, *5*, 4935−4938. (d) Kuramochi, Y.; Satake, A.; Kobuke, Y. *J. Am. Chem. Soc.* **2004**, *126*, 8668−8669. (e) Hwang, I.-W.; Park, M.; Ahn, T. K.; Yoon, Z. S.; Ko, D. M.; Kim, D.; Ito, F.; Ishibashi, Y.; Khan, S. R.; Nagasawa, Y.; Miyasaka, H.; Ikeda, C.; Takahashi, R.; Ogawa, K.; Satake, A.; Kobuke, Y. *Chem.—Eur. J.* **2005**, *11*, 3753−3761.

10.1021/jo060768n CCC: $33.50
Published on Web 06/22/2006

aggregates composed of π-conjugated components is used as a new type of light-harvesting antenna as well as an energy-transfer reagent.[8−10] Shinkai and co-workers reported that an efficient energy transfer takes place from a one-dimensional aggregate composed of an unsubstituted perylenediimide donor to a substituted perylenediimide acceptor incorporated into the aggregate.[8] Meijer and co-workers found that an aggregate composed of oligo(*p*-phenylenevinylene)s with different repeating units provides an attractive energy-transfer medium.[9] In the self-assembled systems, the acceptor molecules, which possess structural similarity with the donor molecules, are efficiently incorporated into the well-defined columnar-type aggregates composed of donor molecules without destabilization of the self-assembled ordering. Thus, study of the one-dimensional aggregates composed of the π-conjugated components is a new attractive task for chemists to develop an artificial light-harvesting system.

Recently, we reported that fluorescent hexaazatriphenylenes (HATs) with six aromatic groups can be self-assembled one-dimensionally in the concentrated solution state to form organogels as well as in the bulk state to form columnar liquid crystals.[11] This finding led us to design and prepare a new type of light-harvesting system based on the HAT-based one-dimensional aggregates. As a result of structural screening in the precedent work, one can find that a combination between a central HAT core and six peripheral biphenyl functional groups plays an important role in constructing the one-dimensional aggregates.[11] However, detailed analysis of the HAT-based aggregates was limited because of the high temperature (>300 °C) in the columnar liquid crystal formation and high concentration in the organogel formation. When the aggregate is formed in a homogeneous organic solution at moderate or dilute concentration, the aggregation behavior would be analyzed conveniently by spectroscopic methods such as UV−vis, fluorescence, and ^{1}H NMR. The desired aggregate would be obtained by introducing alkyl chains into the HAT derivative. The alkyl chains can maintain a subtle balance between HAT−HAT interaction and HAT−solvent interaction to provide the one-dimensional aggregate. In this paper, we report the preparation of HAT derivatives with six alkyl/alkoxy-chain-containing biphenyl groups and their self-assembling nature both in solution and in the film state. Finally, the light-harvesting effect of the HAT-based aggregate system is discussed.

Results and Discussion

Preparation. HATs with six alkyl/alkoxy-chain-containing biphenyl groups (**6a**, 3′,4′-dioctyloxybiphenyl-4-yl; **6b**, 4′-octyloxybiphenyl-4-yl; **6c**, 4′-octylbiphenyl-4-yl; **6d**, 4′-((*S*)-3,7-dimethyloctyloxy)biphenyl-4-yl) were prepared by condensation reactions of the corresponding diaryl diketones **4a**−**d** with hexaaminobenzene **5**[12] (Scheme 1). The key synthetic intermediate diaryl diketones **4a**−**d** were derived from commercially available 4,4′-dibromobenzil (**3**) by Suzuki coupling reactions with the corresponding arylboronic acids **2a**−**d** in the presence of a palladium(0) catalyst. The boronic acids **2a**−**d** were obtained from the corresponding bromides **1a**−**d** by treatment with butyllithium followed with trimethyl borate. In the case of **2b**, the corresponding free boronic acid **2b′** was used without protection with 2,2-dimethyl-1,3-propanediol. HATs **6a**−**d** were characterized on the basis of a spectroscopic method, MALDI-TOF mass spectrometry, and elemental analysis.

HATs **6a**−**d** can dissolve in common organic solvents such as benzene, toluene, dichloromethane, chloroform, and THF. Also, nonpolar solvents (hexane, octane, and cyclohexane) are effective to dissolve **6a**−**d** except for **6b** in hexane and octane. A transparent film of **6a**−**d** can be prepared by a conventional spin-coating technique.

UV−Vis Spectroscopy. π-Stacking interaction constructing the one-dimensional aggregates was confirmed by means of UV−vis spectroscopy. In polar chloroform solutions, **6a**−**d** provides two absorption bands around 410 and 360 nm (Figure 1a, Table 1, and Supporting Information). The two bands are assigned to the transition from the ground state to the $\nu = 0$ level of the lowest excited state (0−0 vibronic transition) and to the $\nu = 1$ level (0−1 vibronic transition), respectively. The spectral pattern with an intense 0−0 transition band and a shoulder-like 0−1 transition band changed scarcely depending on the concentration and temperature, indicating that **6a**−**d** dissolved molecularly in polar chloroform (Figure 1a and Supporting Information).

In contrast, nonpolar hexane and cyclohexane solutions of **6a**−**d** show different spectral patterns with an intense 0−1 transition band and a shoulder-like 0−0 transition band (Figure 1b, Table 1, and Supporting Information). The trend is very similar to those of π-stacked aggregates with an H-type parallel stacking mode,[13] which is rationalized by the molecular exciton model.[14] In **6c**, a concentration- and temperature-dependent UV−vis spectral change was observable in the hexane and octane solutions (Figure 1b and Supporting Information). The absorbance of the 0−0 band around 380 nm increased with decreasing concentration and increasing temperature. The resulting spectra were very similar to those observed in the chloroform

(5) (a) Tsuda, A.; Nakamura, T.; Sakamoto, S.; Yamaguchi, K.; Osuka, A. *Angew. Chem., Int. Ed.* **2002**, *41*, 2817−2821. (b) Hwang, I.-W.; Kamada, T.; Ahn, T. K.; Ko, D. M.; Nakamura, T.; Tsuda, A.; Osuka, A.; Kim, D. *J. Am. Chem. Soc.* **2004**, *126*, 16187−16189.

(6) (a) Hunter, C. A.; Hyde, R. K. *Angew. Chem., Int. Ed. Engl.* **1996**, *35*, 1936−1939. (b) Michelsen, U.; Hunter, C. A. *Angew. Chem., Int. Ed.* **2000**, *39*, 764−767. (c) Haycock, R. A.; Yartsev, A.; Michelsen, U.; Sundstrcm, V.; Hunter, C. A. *Angew. Chem., Int. Ed.* **2000**, *39*, 3616−3619. (d) Haycock, R. A.; Hunter, C. A.; James, D. A.; Michelsen, U.; Sutton L. R. *Org. Lett.* **2000**, *2*, 2435−2438.

(7) (a) Drain, C. M.; Nifiatis, F.; Vasenko, A.; Batteas, J. D. *Angew. Chem., Int. Ed.* **1998**, *37*, 2344−2347. (b) Schugar, H. J. *Angew. Chem., Int. Ed.* **1998**, *37*, 2368−2370. (c) Ikeda, C.; Nagahara, N.; Yoshioka, N.; Inoue, H. *New J. Chem.* **2000**, *24*, 897−902. (d) Rucareanu, S.; Mongin, O.; Schuwey, A.; Hoyler, N.; Gossauer, A.; Amrein, W.; Hediger, H.-U. *J. Org. Chem.* **2001**, *66*, 4973−4988.

(8) Sugiyasu, K.; Fujita, N.; Shinkai, S. *Angew. Chem., Int. Ed.* **2004**, *43*, 1229−1233.

(9) Hoeben, F. J. M.; Herz, L. M.; Daniel, C.; Jonkheijm, P.; Schenning, A. P. H. J.; Silva, C.; Meskers, S. C. J.; Beljonne, D.; Phillips, R. T.; Friend, R. H.; Meijer, E. W. *Angew. Chem., Int. Ed.* **2004**, *43*, 1976−1979.

(10) (a) Sagawa, T.; Fukugawa, S.; Yamada, T.; Ihara, H. *Langmuir* **2002**, *18*, 7223−7228. (b) Ajayaghosh, A.; George, S. J.; Praveen, V. K. *Angew. Chem., Int. Ed.* **2003**, *42*, 332−335. (c) Sugiyasu, K.; Fujita, N.; Takeuchi, M.; Yamada, S.; Shinkai, S. *Org. Biomol. Chem.* **2003**, 895−899. (d) Guerzo, A. D.; Olive, A. G. L.; Reichwagen, J.; Hoph, H.; Desvergne, J.-P. *J. Am. Chem. Soc.* **2005**, *127*, 17984−17985.

(11) Ishi-i, T.; Hirayama, T.; Murakami, K.; Tashiro, H.; Thiemann, T.; Kubo, K.; Mori, A.; Yamasaki, S.; Akao, T.; Tsuboyama, A.; Mukaide, T.; Ueno, K.; Mataka, S. *Langmuir* **2005**, *21*, 1261−1268.

(12) (a) Mataka, S.; Eguchi, H.; Takahashi, K.; Hatta, T.; Tashiro, M. *Bull. Chem. Soc. Jpn.* **1989**, *62*, 3127−3131. (b) Mataka, S.; Shimojyo, Y.; Hashimoto, I.; Tashiro, M. *Liebigs Ann.* **1995**, 1823−1825. (c) Komin, A. P.; Carmack, M. *J. Heterocycl. Chem.* **1975**, *12*, 829−833.

(13) (a) van der Boom, T.; Hayes, R. T.; Patrick, Y. Z.; Bushard, J.; Weiss, E. A.; Wasielewski, M. R. *J. Am.Chem. Soc.* **2002**, *124*, 9582−9590. (b) Wang, W.; Han, J. J.; Wang, L.-Q.; Li, L.-S.; Shaw, W. J.; Li, A. D. Q. *Nano Lett.* **2004**, *3*, 455−458.

(14) Kasha, M.; Rawls, H. R.; El-Bayoumi, M. A. *Pure Appl. Chem.* **1965**, *11*, 371−392.

SCHEME 1. Preparation of HATs Having Alkyl Side Chains, 6a−d

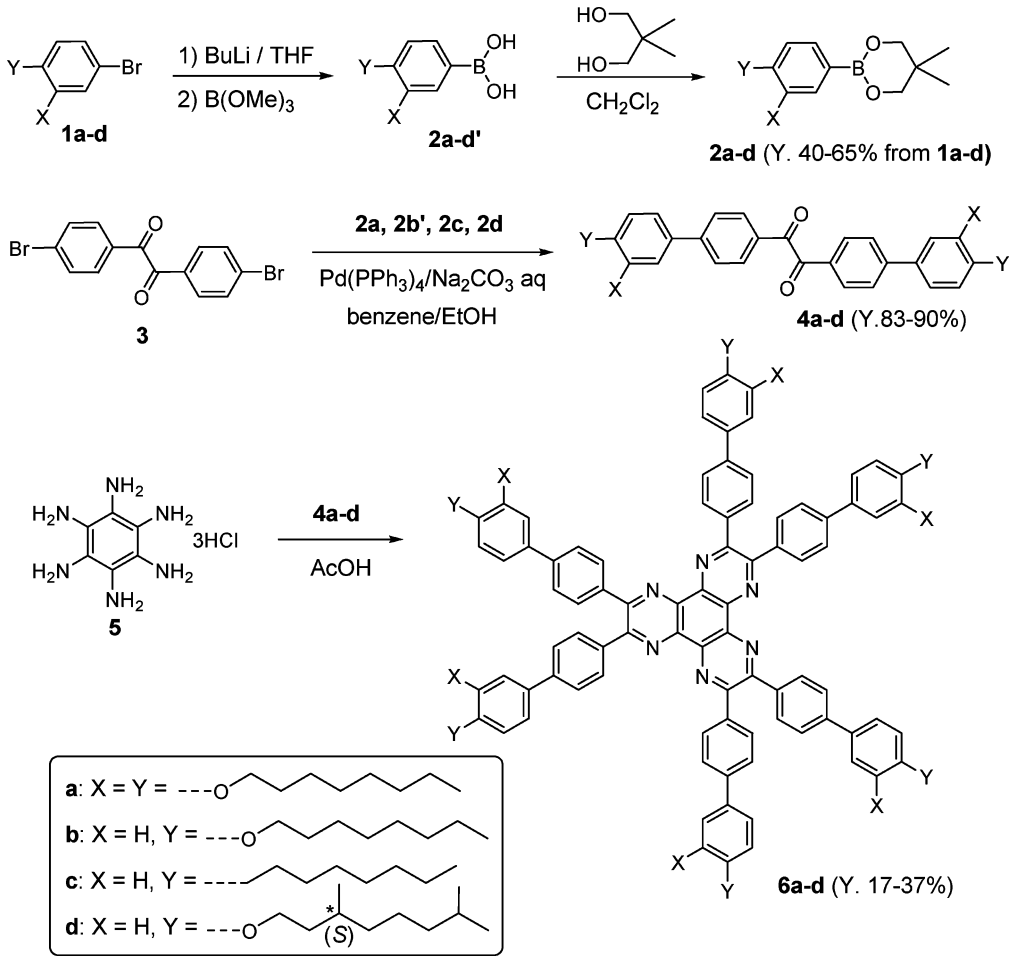

solutions. The phenomena are attributed to the dynamic exchange between the monomer and the aggregate species.

In hexane, a comparison between the concentration dependence of **6a**, **6c**, and **6d** indicates the order of aggregate stability to be **6a** > **6d** > **6c** (Figure 1a and Supporting Information). In cyclohexane, the concentration dependence of **6b** is smaller than that of **6a** (Supporting Information). As a summary of the foregoing results, one can conclude that the order of aggregate stability is **6b** > **6a** > **6d** > **6c**. Compared to alkyl-chain-containing HAT **6c**, alkoxy-chain-containing HATs **6a**, **6b**, and **6d** provide superior aggregative nature, which would be attributed to the expansion of the π-system including oxygen atoms. Among the alkoxy-chain-containing HATs, the low stability of **6d** would be ascribed to unfavored packing of the chiral alkyl groups arising from the branched structure.[15] Compared to **6b** with six octyloxy groups, **6a** with twelve octyloxy groups seems to show more favorable solvation to decrease the aggregative nature.

The chirality in **6d** is reflected in CD spectra in hexane (Supporting Information). Under the aggregated conditions of 0.1−1.0 mM hexane solution at 20 °C, Cotton effects are observable around the absorption maxima, although the magnitude is small. In contrast, such Cotton effects could not be observed in polar chloroform solution. The results suggest that the aggregate of **6d** takes a helix stacking mode to make a left-handed or right-handed helix.[11]

The aggregate structure formed in nonpolar solvent can be preserved in the film state. For example, the spin-coating film of **6b** obtained from a cyclohexane solution provides an intense 0−1 band around 360 nm in the UV−vis spectrum (Figure 2). The spectral pattern is very similar to that of the aggregated **6b** in the cyclohexane solution. The result shows that in the film state the **6b** molecules are self-assembled to preserve the H-aggregate stacking mode created in the nonpolar cyclohexane solution. In contrast, another spin-coating film obtained from a polar chloroform solution, in which **6b** dissolves molecularly, provides a nonaggregated spectral pattern with an intense 0−0 band around 400 nm (Figure 2). Similar aggregation behavior in the film state was observed in **6a**, **6c**, and **6d**.

Fluorescence Spectroscopy. The aggregation of **6a−d** is reflected in steady-state fluorescence spectra. In chloroform, the emission band around 460 nm in **6c** changed scarcely depending on the concentration (Figure 3b). In contrast, in hexane solutions of **6c**, the emission band is shifted bathochromically from 434 to 471 nm with increasing concentration (from 0.001 to 1.0 mM), according to facilitated aggregation (Figure 3a and Table 1). The emission band (471 nm) in a 1.0 mM hexane solution of **6c** is observed at longer wavelength than that (461 nm) in 1.0 mM chloroform solution; nevertheless, the polarity of hexane is lower than that of chloroform. The bathochromic shift observed in hexane solutions would be attributed to a stabilization effect on the excited state in the aggregates.[16] Probably,

(15) Kastler, M.; Pisula, W.; Wasserfallen, D.; Pakula, T.; Müllen, K. *J. Am. Chem. Soc*. **2005**, *127*, 4286−4296.

(16) Ikeda, M.; Takeuchi, M.; Shinkai, S. *Chem. Commun*. **2003**, 1354−1355.

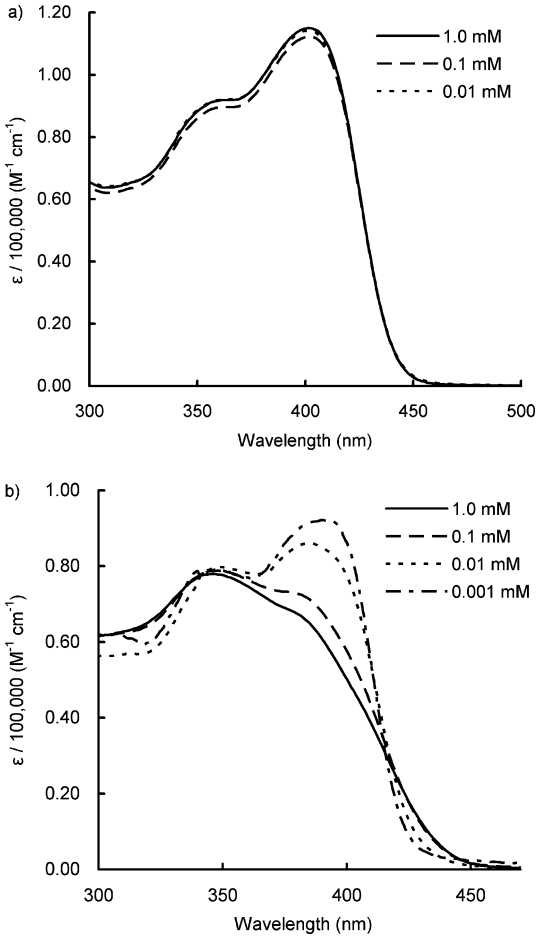

FIGURE 1. UV−vis spectra of **6c** in (a) chloroform and (b) hexane at 20 °C at 0.001, 0.01, 0.1, and 1.0 mM.

TABLE 1. UV−Vis and Fluorescence Spectral Data for 6a, 6b, 6c, and 6d at 20 °C

compd	solvent	concn (mM)	λ_{max} (nm) (ϵ (M^{-1} cm^{-1}))	λ_{FL} (nm)
6a	hexane	1.0	356 (sh, 71000), 386 (sh, 65000)	497
		0.1	356 (71000), 386 (sh, 67000)	492
		0.01	356 (71000), 386 (sh, 69000)	487
	cyclohexane	1.0	363 (sh, 85000), 388 (87000)	
		0.1	363 (sh, 85000), 390 (90000)	
		0.01	363 (sh, 85000), 401 (98000)	
	chloroform	1.0	370 (sh, 87000), 409 (100000)	504
		0.01	370 (sh, 87000), 409 (100000)	504
6b	cyclohexane	1.0	349 (78000), 385 (sh, 71000)	482
		0.1	354 (79000), 386 (78000)	472
		0.01	357 (81000), 391 (86000)	462
	chloroform	1.0	362 (sh, 90000), 406 (110000)	479
		0.01	362 (sh, 93000), 406 (110000)	479
6c	hexane	1.0	344 (78000), 378 (sh, 68000)	471
		0.1	345 (79000), 381 (sh, 73000)	464
		0.01	344 (79000), 385 (86000)	456
		0.001	345 (79000), 390 (92000)	434
	chloroform	1.0	362 (sh, 90000), 406 (110000)	461
		0.01	362 (sh, 93000), 406 (110000)	461
6d	hexane	1.0	347 (82000), 382 (sh, 71000)	481
		0.1	347 (82000), 382 (sh, 73000)	477
		0.01	347 (82000), 387 (79000)	471
	chloroform	1.0	363 (sh, 73000), 406 (90000)	480
		0.01	363 (sh, 73000), 406 (90000)	480

the stabilization effect is ascribed to the migration of the photogenerated exciton or the excimer formation in the aggregate structures.[17] Similar concentration-dependent emission behavior was observable in **6a**, **6b**, and **6d** (Table 1 and Supporting Information). The order of the concentration-dependent fluorescence spectral change in **6a**−**d** is in accordance with that of the UV−vis spectral change, indicating again the order of aggregate stability to be **6b** > **6a** > **6d** > **6c**.

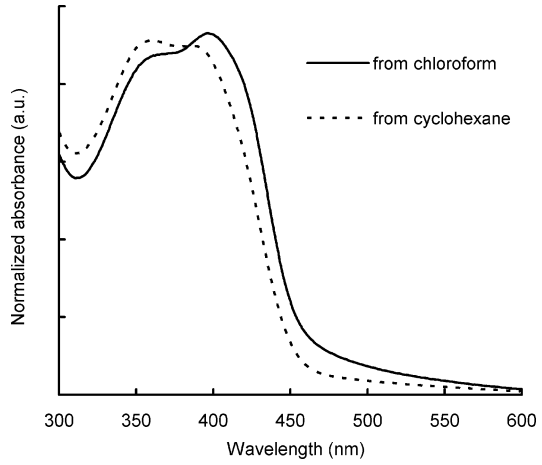

FIGURE 2. UV−vis spectra of the spin-coating films of **6b** obtained from chloroform and cyclohexane solutions (5 mM).

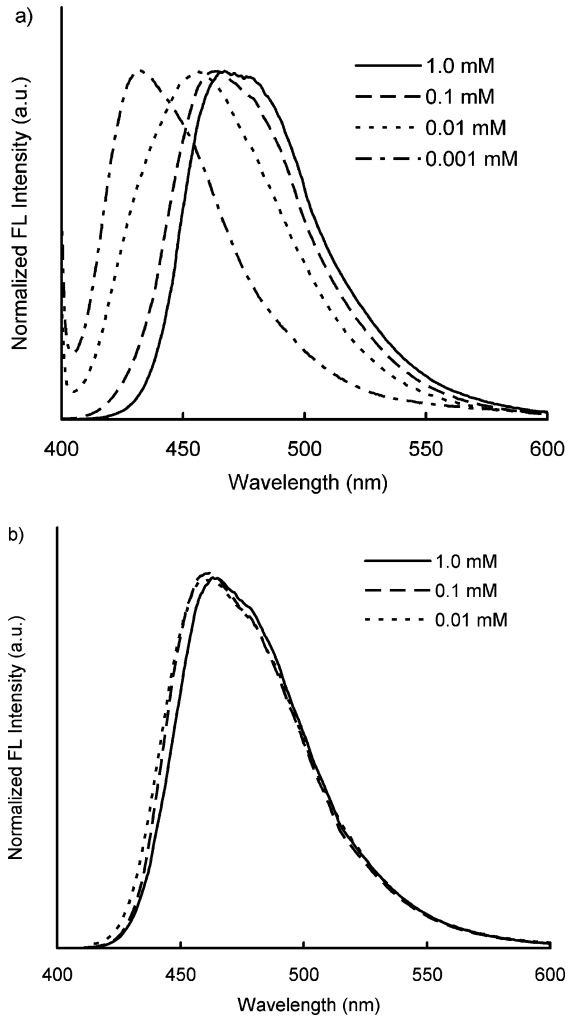

FIGURE 3. Steady-state fluorescence spectra of **6c** at 20 °C in (a) hexane (λ_{ex} = 391 nm) and (b) chloroform (λ_{ex} = 403 nm) at 0.001, 0.01, 0.1, and 1.0 mM.

In chloroform solutions, **6a**−**d** provide moderate fluorescence quantum yields (Φ_{FL}) of 0.54−0.60. The Φ_{FL} values are reduced

TABLE 2. Fluorescence Quantum Yields (Φ_{FL}) for 6a, 6b, 6c, and 6d[a]

	Φ_{FL}		
compd	hexane	cyclohexane	chloroform
6a	0.39	0.54	0.60
6b		0.47	0.60
6c	0.21	0.32	0.54
6d	0.36	0.46	0.60

[a] Relative to quinine bisulfate (0.55).

in nonpolar hexane (0.21−0.39) and cyclohexane (0.32−0.54) solutions (Table 2); nevertheless, the polarity of hexane and cyclohexane is smaller than that of chloroform. The lowering emission ability is also supportive of the aggregation of **6a**−**d** in the nonpolar solvents.

The stabilization of the excited state in the aggregates of **6a**−**d** would be supported by time-resolved fluorescence spectra. For a dilute 0.001 mM hexane solution of **6c**, the decay curve at 487 nm was fitted to a double exponential with lifetimes of 0.36 ns (89%) and 1.60 ns (11%). The shorter lifetime with 89% population suggests that the monomer species of **6c** exists mainly at the dilute 0.001 mM concentration. At a high concentration of 1.0 mM, the populations of the two lifetimes are inverted to be 14% (0.57 ns) and 86% (2.22 ns), according to facilitated aggregation.[18,19] The difference in both the shorter and longer lifetimes (0.36 ns versus 0.57 ns for the short lifetime and 1.60 ns versus 2.22 ns for the long lifetime) is likely due to the error introduced by the assumption that decay is fitted with only two distinct lifetimes. Theoretically, the decay is more complicated and is fitted to a multiple exponential, because the aggregates have size and length distributions.[17,18] However, it can be emphasized that the aggregates obtained at higher concentration include more long-lived species compared to those obtained at lower concentration, indicating that the aggregation is facilitated with increasing concentration. Similarly, fluorescence decays of **6a** in hexane and **6b** in cyclohexane were fitted with a double exponential, and a long-lived species was given at high concentration, although the trend of lifetime populations was not straightforward such as that of **6c** arising from the analysis error (Supporting Information).

^{1}H NMR Spectroscopy. In the ^{1}H NMR spectra, a line-broadening effect arising from the π-stacked aggregation was observed in **6a**−**c** in octane-d_{18} and cyclohexane-d_{12}. The chemical shifts and the shape of the broad resonances are dependent on the concentration and temperature, indicating the dynamic exchange between the monomer and aggregate species. Typical examples of **6c** in octane-d_{18} at 20 and 100 °C are shown in Figure 4. At high concentration (∼1.0 mM) the proton signals appeared in a higher magnetic field compared to those at dilute concentration (∼0.0005 mM). The higher magnetic field shift is ascribed to the π-stacking among the HAT core moieties.[11]

The chemical shifts for the $ArOCH_2$ proton for **6b** and the $ArCH_2$ proton for **6c** were plotted against the concentration (Figure 5). For **6a**, the chemical shifts for the $ArOCH_2$ protons could not be checked because of the overlap for the two types

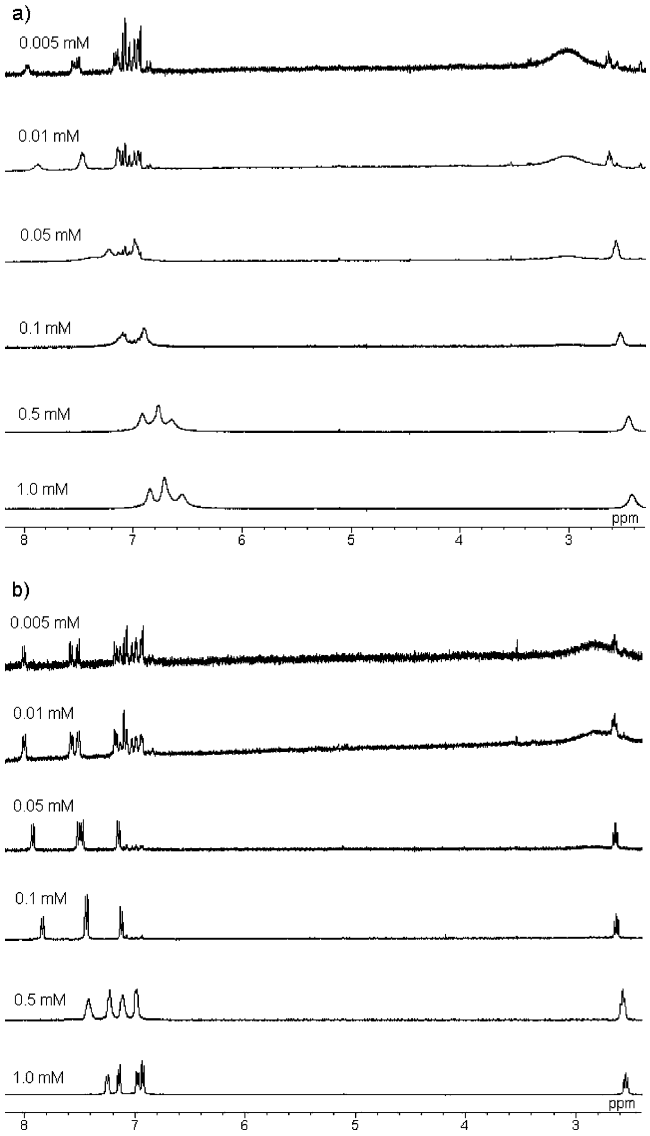

FIGURE 4. ^{1}H NMR spectra of **6c** in octane-d_{18} at 0.005, 0.01, 0.05, 0.1, 0.5, and 1.0 mM: (a) at 20 °C and (b) at 100 °C.

of $ArOCH_2$ proton signals. The concentration dependence at 20 °C can be analyzed by an infinite association model,[20] by which the self-association constant (K) was estimated (Table 3). In cyclohexane-d_{12} at 20 °C, the K value (74300 M^{-1}) of **6b** is larger by 1 order of magnitude than that (5750 M^{-1}) of **6c**, indicating the superior aggregative nature of **6b**. In **6c**, the K value (10500 M^{-1}) in octane-d_{18} is 2 times larger than that (5750 M^{-1}) in cyclohexane-d_{12}.

In octane-d_{18} solutions of **6c**, the K values were obtained at different temperatures in the range of 20−100 °C (Figure 6 and Table 3). The thermodynamic parameters for the self-association were estimated by the van't Hoff plot. The obtained $\Delta H°$ (−29.3 kJ mol^{-1}) and $\Delta S°$ (−22.8 J mol^{-1} K^{-1}) values seem to indicate an entropically driven self-association. Probably, the **6a**−**d**

(17) Wu, J.; Fechtenkötter, A.; Gauss, J.; Watson, M. D.; Kastler, M.; Fechtenkötter, C.; Wagner, M.; Müllen, K. *J. Am. Chem. Soc.* **2004**, *126*, 11311−11321.
(18) Nguyen, T.-Q.; Martel, R.; Avouris, P.; Bushey, M. L.; Brus, L.; Nuckolls, C. *J. Am. Chem. Soc.* **2004**, *126*, 5234−5242.
(19) Ryu, S. Y.; Kim, S.; Seo, J.; Kim, Y.-W.; Kwon, O.-H.; Jang, D.-J.; Park, S. Y. *Chem. Commun.* **2004**, 70−71.
(20) (a) Shetty, A. S.; Zhang, J.; Moore, J. S. *J. Am. Chem. Soc.* **1996**, *118*, 1019−1027. (b) Lahiri, S.; Thompson, J. L.; Moore, J. S. *J. Am. Chem. Soc.* **2000**, *122*, 11315−11319. (c) Tobe, Y.; Utsumi, N.; Kawabata, K.; Nagano, A.; Adachi, K.; Araki, S.; Sonoda, M.; Hirose, K.; Naemura, K. *J. Am. Chem. Soc.* **2002**, *124*, 5350−5364. (d) Kobayashi, K.; Kobayashi, N. *J. Org. Chem.* **2004**, *69*, 2487−2497. (e) Sugiura, H.; Takahira, Y.; Yamaguchi, M. *J. Org. Chem.* **2005**, *70*, 5698−5708.

TABLE 3. Association Constants (K)[a] and Thermodynamic Parameters[b] for Self-Aggregation of 6b and 6c

compd	solvent	K (M^{-1}) 20 °C	40 °C	60 °C	80 °C	100 °C	$\Delta H°$ (kJ mol^{-1})	$\Delta S°$ (J mol^{-1} K^{-1})
6b	cyclohexane-d_{12}	74300						
6c	cyclohexane-d_{12}	5750						
6c	octane-d_{18}	10500	5400	2400	1400	840	−29.3	−22.8

[a] Determined on the basis of the infinite model by nonlinear least-squares fitting of chemical shift data.[20] The experimental uncertainty of the K value amounts to about ±5−10%. All the correlation coefficients were >0.99. [b] Determined by the van't Hoff plot. The correlation coefficient was 0.999.

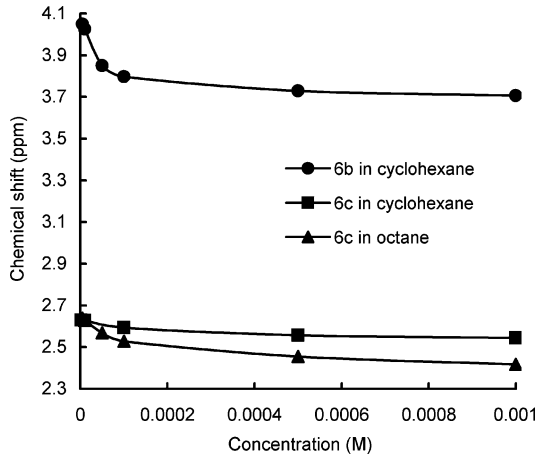

FIGURE 5. Chemical shift vs concentration for **6b** ($ArOCH_2$ proton) in cyclohexane-d_{12} and **6c** ($ArCH_2$ proton) in cyclohexane-d_{12} and in octane-d_{18} at 20 °C.

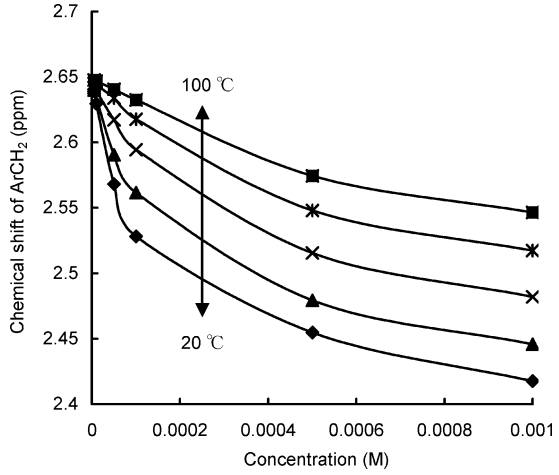

FIGURE 6. Chemical shift vs concentration for **6c** in octane-d_{18} at 20, 40, 60, 80, and 100 °C.

molecules are self-assembled mainly by π-stacking interactions in the central HAT core in nonpolar solvent.

Light Harvesting. As described above, fluorescent HAT derivatives **6a**−**d** form one-dimensional aggregates both in solution and in the film state. To apply these fluorescent aggregates to a light-harvesting antenna, we selected HAT derivative **7** with six perylenediimide (PDI) moieties as an energy-acceptor molecule (Chart 1). In a precedent study, we have reported that **7** is self-assembled both in solution and in the film state to form a highly stabilized dimer aggregate, in which an efficient energy transfer occurs from the HAT core to the PDI moiety.[21] These results provide the valuable information that an efficient light-harvesting system can be created when the dimer of **7** is incorporated into the aggregate

CHART 1. Molecular Structure of 7 and 8 as a Light-Harvesting Acceptor and Donor, Respectively

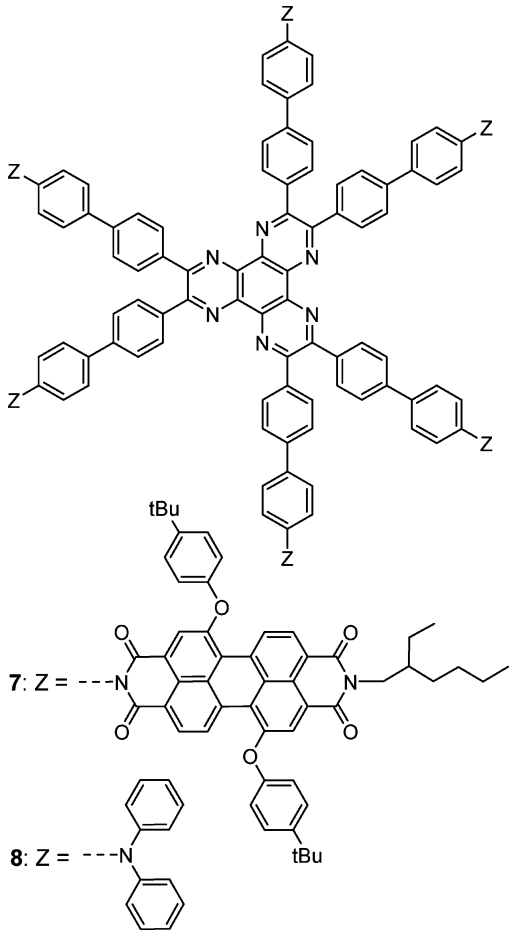

of **6**. In addition, **7** also acts as an electron acceptor to generate charge separation when HAT derivative **8**[11] with six electron-rich triphenylamino (TPA) moieties is used as an electron-donor molecule (Chart 1). Here, we selected HAT **6b** as a light-harvesting antenna as well as an energy-transfer reagent, because **6b** has the most superior aggregative nature among **6a**−**d**.

A film sample of **6b** doped with 5 mol % **7** (100:5 mixture of **6b**/**7**) was prepared by spin coating from a cyclohexane solution, and the energy transfer from the **6b**-based aggregate to **7** incorporated into the aggregate was examined. The spin-coating samples provide a clear overlap of the fluorescence spectrum of **6b** and the absorption spectrum of **7** (Supporting Information). In the precedent artificial light-harvesting systems based on the self-assembled one-dimensional aggregates, quantitative analysis of the energy transfer was difficult due to significant overlap between donor and acceptor emissions,

(21) Ishi-i, T.; Murakami, K.; Imai, Y.; Mataka, S. *Org. Lett.* **2005**, *7*, 3175−3178.

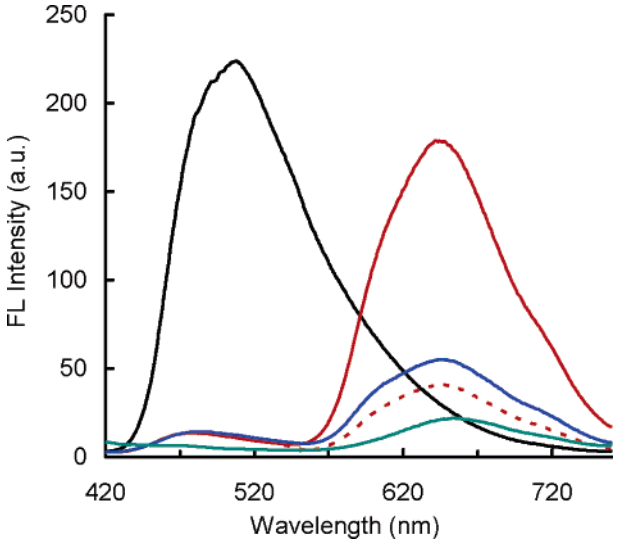

FIGURE 7. Fluorescence spectra excited at the HAT chromophore (395 nm) of **6a**/**7**/**8** mixtures with 100:0:0 (black line), 100:5:0 (red line), 100:5:5 (blue line), and 0:0:5 (green line) molar ratios in the spin-coating film (from cyclohexane solution) at 20 °C. The fluorescence spectrum of the 100:5:0 mixture excited at the PDI chromophore (at 517 nm) is indicated by a dotted red line.

because the donor and acceptor components have similar structural features such as perylenediimides with different substituents and oligo(*p*-phenylenevinylene)s with different repeating units.[8,9] On the other hand, the present system has a versatile advantage of good separation between the donor and acceptor emissions, because of the structural difference of the donor HAT and the acceptor PDI moieties.

In the presence of **7**, the emission from **6b** around 510 nm was quenched significantly even upon excitation of the HAT chromophore (Figure 7). In addition, the PDI emission around 650 nm upon indirect excitation of the HAT chromophore is enhanced by a factor of 4 compared to that observed upon direct excitation of the PDI chromophore, indicating the light-harvesting effect of the **6b**-based aggregate (Figure 7). A good energy transfer efficiency of ca. 80% can be estimated on the basis of a comparison between absorption and excitation spectra (Supporting Information). When the spin-coating film was prepared from polar chloroform solutions including molecularly dissolved **6b**, the light-harvesting effect was reduced significantly (Supporting Information), suggesting the importance of the **6b**-based aggregate as a good light-harvesting antenna as well as an energy transfer reagent.

The enhanced HAT emission in the 100:5 mixture of **6b**/**7** is reduced to one-third, when 5 mol % **8** is newly doped as an electron donor (Figure 7). The result suggests that in the 100:5:5 mixture of **6b**/**7**/**8**, an electron transfer takes place from the excited state of the PDI moiety in **7**, generating an ion pair of the PDI anion radical in **7** and the TPA cation radical in **8**.[22,23] The energy transfer and subsequent electron transfer phenomena were easily visualized by a change in the emission color from brilliant green HAT emission to brilliant red PDI emission and after very weak PDI emission (Figure 8).

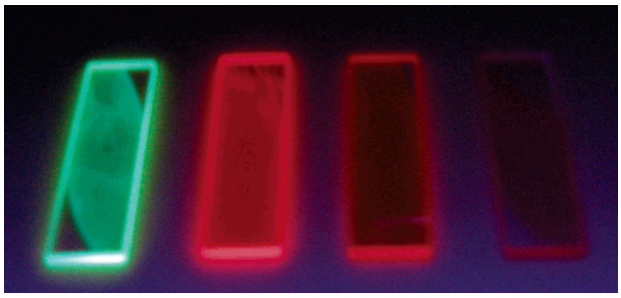

FIGURE 8. Fluorescent images under UV light (365 nm) for **6a**/**7**/**8** mixtures with 100:0:0, 100:5:0, 100:5:5, and 0:0:5 molar ratios (from left to right) in the spin-coating film.

Conclusion

In conclusion, we have demonstrated that hexaazatriphenylenes with six alkyl- and alkoxy-chain-containing biphenyl groups can be self-assembled to form one-dimensional aggregates both in solution and in the film state. The aggregation of the hexaazatriphenylene molecules is mainly stabilized by the π-stacking of the central aromatic core. The aggregation ability highly depends on the nature of the alkyl and alkoxy chains at the peripheral positions. Fluorescence spectroscopy is a useful method to study the aggregation. According to facilitated aggregation, the emission band shifts to a longer wavelength region together with reduction of the fluorescence quantum yield as well as an increase of the fluorescence lifetime.

The self-assembled fluorescent hexaazatriphenylene can be developed to an artificial light-harvesting antenna as well as an energy-transfer reagent. When a hexaazatriphenylene derivative having an energy- and electron-accepting perylenediimide moiety is doped with the fluorescent hexaazatriphenylene aggregate, an efficient energy transfer takes place from the aggregate to the acceptor moiety. Further, by the combination with the hexaazatriphenylene derivative having an electron-donating triphenylamino moiety, an electron transfer can be achieved between the donor and acceptor moieties in the self-assembled aggregate system. We believe that the present study will provide valuable new information not only for creation of one-dimensional architectures but also for artificial light-harvesting systems.

Experimental Section

Spectroscopic Measurement. UV−vis spectra were measured in a 0.01 cm width quartz cell (1.0 mM), a 0.1 cm cell (0.1 mM), a 1.0 cm cell (0.01 mM), and a 10.0 cm cell (0.001 mM). Fluorescence spectra were measured in a 1.0 cm width quartz cell. Time-resolved fluorescence spectra were measured by a single-photon-counting method with a nitrogen-filled nanosecond flash lamp (pulse width of 1 ns, pulse repetition rate of 40 Hz).

Preparation of Spin-Coating Films. Film samples for the measurements of UV−vis and fluorescence spectroscopy were prepared by drop casting and subsequent spin coating (2000 rpm, 30 s) from cyclohexane or chloroform solutions on a quartz cell (12.5 × 12.5 × 45 mm). The 100:0:0 molar ratio sample was obtained from a 5.0 mM cyclohexane solution (50 μL) of **6b**, the 100:5:0 molar ratio sample from a cyclohexane solution (50 μL) including 5.0 mM **6b** and 0.25 mM **7**, the 100:5:5 molar ratio sample from a cyclohexane solution (50 μL) including 5.0 mM **6b**, 0.25 mM **7**, and 0.25 mM **8**, and the 0:5:0 molar ratio sample from a 0.25 mM chloroform solution (50 μL) of **7**.

General Procedure for Preparation of 2,2-Dimethyl-1,3-propanediol 3,4-Bis(octyloxy)phenylboronate (2a). To a solution

(22) Schmidt-Mende, L.; Fechtenkötter, A.; Müllen, K.; Moons, E.; Friend, R. H.; MacKenzie, J. D. *Science* **2001**, *293*, 1119−1122.
(23) Sandanayaka, S. D. A.; Matsukawa, K.; Ishi-i, T.; Mataka, S.; Araki, Y.; Ito, O. *J. Phys. Chem. B* **2004**, *108*, 19995−20004.

of **1a** (921 mg, 2.3 mmol) in dry THF (10 mL) was added dropwise 1.58 M *n*-butyllithium/hexane solution (1.7 mL, 2.7 mmol) at −78 °C for 15 min under an argon atmosphere. After the mixture was stirred at −78 °C for 0.5 h, trimethyl borate (340 μL, 3.0 mmol) was added dropwise for 15 min to the mixture. The mixture was stirred at −78 °C for 1 h and warmed to room temperature. After the reaction mixture was quenched with aqueous 1.2 M hydrochloric acid solution (to pH 5−7), it was extracted with diethyl ether. The combined organic layers were washed with brine, dried over anhydrous magnesium sulfate, and evaporated in vacuo to dryness. The residue (760 mg) and 2,2-dimethyl-1,3-propanediol (208 mg, 2.0 mmol) were dissolved in dichloromethane (20 mL), and the resulting solution was stirred at room temperature for 2 h under an argon atmosphere. After the evaporation, the residue was purified by silica gel column chromatography (KANTO 60N) eluting with dichloromethane/hexane (2:3, v/v) to give **2a** in 40% yield (411 mg, 0.92 mmol) as a colorless oil: IR (KBr, cm^{-1}) 2927, 1598, 1476, 1420, 1317 (ν_{B-O}), 1261, 1233, 1138; ^1H NMR ($CDCl_3$) δ 0.88 (t, J = 6.6 Hz, 6 H), 1.02 (s, 6 H), 1.28−1.54 (m, 20 H), 1.81 (quint, J = 6.6 Hz, 4 H), 3.75 (s, 4 H), 4.01 (t, J = 6.6 Hz, 2 H), 4.02 (t, J = 6.6 Hz, 2 H), 6.86 (d, J = 7.9 Hz, 1 H), 7.30 (d, J = 2.3 Hz, 1 H), 7.36 (dd, J = 2.3, 7.9 Hz, 1 H); FAB-MS (positive, NBA) *m/z* 446 (M^+); HR-MS (EI, positive) *m/z* calcd for $C_{27}H_{47}O_4B$ 446.3567, found 446.3571 (M^+).

Data for 4-octyloxyphenylboronic acid (2b′): white solid; ^1H NMR ($CDCl_3$) δ 0.89 (t, J = 6.6 Hz, 3 H), 1.25−1.55 (m, 10 H), 1.72−1.88 (m, 2 H), 4,05 (t, J = 6.6 Hz, 2 H), 7.00 (d, J = 7.5 Hz, 2 H), 8.14 (d, J = 7.5 Hz, 2 H).

Data for 2,2-dimethyl-1,3-propanediol 4-octylphenylboronate (2c): white needles; mp 44−46 °C; IR (KBr, cm^{-1}) 2925, 1611, 1480, 1419, 1379, 1307 (ν_{B-O}), 1248, 1131; ^1H NMR ($CDCl_3$) δ 0.87 (t, J = 6.3 Hz, 3 H), 1.02 (s, 6 H), 1.26−1.28 (m, 10 H), 1.60 (quint, J = 7.3 Hz, 2 H), 2.60 (t, J = 7.3 Hz, 2 H), 3.76 (s, 4 H), 7.17 (d, J = 7.9 Hz, 2 H), 7.71 (d, J = 7.9 Hz, 2 H); FAB-MS (positive, NBA) *m/z* 302 (M^+). Anal. Calcd for $C_{19}H_{31}BO_2$: C, 75.50; H, 10.34. Found: C, 75.59; H, 10.30.

Data for 2,2-dimethyl-1,3-propanediol 4-{(*S*)-3,7-dimethyloctyloxy}phenylboronate (2d): colorless oil; IR (KBr, cm^{-1}); 2959, 1602, 1568, 1344, 1318 (ν_{B-O}), 1173, 1132, 1019; ^1H NMR ($CDCl_3$) δ 0.86 (d, J = 6.6 Hz, 6 H), 0.93 (d, J = 6.4 Hz, 3 H), 1.00 (s, 6 H), 1.13−1.83 (m, 10 H), 3.74 (s, 4 H), 4.00 (t, J = 6.4 Hz, 2 H), 6.86 (d, J = 8.7 Hz, 2 H), 7.71 (d, J = 8.7 Hz, 2 H); FAB-MS (positive, NBA) *m/z* 346 (M^+); HR-MS (EI, positive) *m/z* calcd for $C_{21}H_{35}O_3B$ 346.2683, found 346.2681 (M^+).

General Procedure for Preparation of Bis{3′,4′-dioctyloxybiphenyl-4-yl)ethanedione (4a). To a mixture of **3** (301 mg, 0.82 mmol) and tetrakis(triphenylphosphine)palladium(0) (60 mg, 0.05 mmol, 3 mol %) in benzene (32 mL) were added **2a** (822 mg, 1.80 mmol), ethanol (8 mL), and aqueous 2 M sodium carbonate solution (16 mL) at 60 °C under an argon atmosphere, and the resulting mixture was heated at 80 °C for 18 h. The reaction mixture was poured into water and extracted with chloroform. The organic layer was washed with brine, dried over anhydrous magnesium sulfate, and evaporated in vacuo to dryness. The residue was purified by silica gel column chromatography (WAKO C300) eluting with chloroform/hexane (1:1, v/v) to give **4a** in 90% yield (644 mg, 0.74 mmol) as an orange powder: mp 108−111 °C; IR (KBr, cm^{-1}) 2922, 1668 ($\nu_{C=O}$), 1597, 1523, 1257, 1205, 1176, 1141, 835, 813; ^1H NMR ($CDCl_3$) δ 0.88 (t, J = 6.6 Hz, 12 H), 1.29−1.55 (m, 40 H), 1.85 (quint, J = 6.6 Hz, 8 H), 4.05 (t, J = 6.6 Hz, 4 H), 4.06 (t, J = 6.6 Hz, 4 H), 6.96 (d, J = 8.3 Hz, 2 H), 7.15 (d, J = 2.3 Hz, 2 H), 7.18 (dd, J = 2.3, 8.3 Hz, 2 H), 7.70 (d, J = 8.6 Hz, 4 H), 8.03 (d, J = 8.6 Hz, 4 H); FAB-MS (positive, NBA) *m/z* 875 [$(M + 1)^+$]. Anal. Calcd for $C_{58}H_{82}O_6$: C, 79.59; H, 9.44. Found: C, 79.59; H, 9.46.

Data for bis(4′-octyloxybiphenyl-4-yl)ethanedione (4b): yellow powder; mp 157−158 °C; IR (KBr, cm^{-1}) 2954, 2921, 2856, 1666 ($\nu_{C=O}$), 1598, 1189, 827, 817; ^1H NMR ($CDCl_3$) δ 0.89 (t, J = 6.6 Hz, 6 H), 1.20−1.55 (m, 20 H), 1.81 (quint, J = 6.6 Hz, 4 H), 4.00 (t, J = 6.6 Hz, 4 H), 7.13 (d, J = 8.3 Hz, 4 H), 7.57 (d, J = 8.3 Hz, 4 H), 7.70 (d, J = 8.3 Hz, 4 H, ArH), 8.03 (d, J = 8.3 Hz, 4 H, ArH); FAB-MS (positive, NBA) *m/z* 619 [$(M + 1)^+$]. Anal. Calcd for $C_{42}H_{50}O_4$: C, 81.51; H, 8.14. Found: C, 81.45; H, 8.13.

Data for bis(4′-octylbiphenyl-4-yl)ethanedione (4c): yellow powder; mp 122−124 °C; IR (KBr, cm^{-1}) 2921, 2851, 1660 ($\nu_{C=O}$), 1601, 1180, 881; ^1H NMR ($CDCl_3$) δ 0.88 (t, J = 6.9 Hz, 6 H), 1.18−1.32 (m, 20 H), 1.65 (quint, J = 7.9 Hz, 4 H), 2.66 (t, J = 7.9 Hz, 4 H), 7.29 (d, J = 8.6 Hz, 4 H), 7.56 (d, J = 8.6 Hz, 4 H), 7.73 (d, J = 8.6 Hz, 4 H), 8.06 (d, J = 8.6 Hz, 4 H); FAB-MS (positive, NBA) *m/z* 587 [$(M + 1)^+$]. Anal. Calcd for $C_{42}H_{50}O_2$: C, 85.96; H, 8.59. Found: C, 85.92; H, 8.58.

Data for bis{4′-[(*S*)-3,7-dimethyloctyloxy]biphenyl-4-yl}-ethanedione (4d): white powder; mp 102−104 °C; IR (KBr, cm^{-1}) 2925, 1677, 1660 ($\nu_{C=O}$), 1600, 1249, 1184, 828; ^1H NMR ($CDCl_3$) δ 0.87 (d, J = 6.6 Hz, 12 H), 0.96 (d, J = 6.3 Hz, 6 H), 1.15−1.87 (m, 20 H), 4.05 (t, J = 6.6 Hz, 4 H), 6.99 (d, J = 8.6 Hz, 4 H), 7.58 (d, J = 8.6 Hz, 4 H), 7.70 (d, J = 8.3 Hz, 4 H), 8.04 (d, J = 8.3 Hz, 4 H); FAB-MS (positive, NBA) *m/z* 675 [$(M + 1)^+$]. Anal. Calcd for $C_{46}H_{58}O_4$: C, 81.86; H, 8.66. Found: C, 81.68; H, 8.64.

General Procedure for Preparation of 2,3,6,7,10,11-Hexakis-{3′,4′-dioctyloxybiphenyl-4-yl}-1,4,5,8,9,12-hexaazatriphenylene (6a). A mixture of hexaaminobenzene trihydrochloride (5) (13 mg, 0.047 mmol) and 4a (123 mg, 0.14 mmol) in acetic acid (5 mL) was heated at the refluxing temperature for 17 h under an argon atmosphere. After the reaction mixture was cooled to room temperature, it was poured into water and extracted with chloroform. The combined organic layers were washed with saturated aqueous sodium hydrogen carbonate solution and with brine, dried over anhydrous magnesium sulfate, and evaporated in vacuo to dryness. The residue was separated by silica gel chromatography (WAKO C300) eluting with chloroform/hexane (1:2, v/v) and by GPC (polystyrene JAIGEL-1H and 2H) eluting with chloroform to give 6a in 35% yield (44 mg, 0.016 mmol) as a glassy brown solid: mp > 250 °C dec; IR (KBr, cm^{-1}) 2924, 2854, 1604, 1500, 1365, 1250, 1142; ^1H NMR ($CDCl_3$) δ 0.88 (t, J = 6.6 Hz, 36 H), 1.29−1.55 (m, 120 H), 1.85 (quint, J = 6.6 Hz, 24 H), 4.06 (t, J = 6.6 Hz, 12 H), 4.08 (t, J = 6.6 Hz, 12 H), 6.96 (d, J = 8.3 Hz, 6 H), 7.21−7.26 (m, 12 H), 7.65 (d, J = 8.6 Hz, 12 H), 8.00 (d, J = 8.6 Hz, 12 H); MALDI-TOF-MS (positive, dithranol) *m/z* 2685.00 [M^+, calcd for $C_{180}H_{246}N_6O_{12}$ 2684.89]. Anal. Calcd for $C_{180}H_{246}N_6O_{12}$: C, 80.49; H, 9.23; N, 3.13. Found: C, 80.26; H, 9.11; N 3.13.

Data for 2,3,6,7,10,11-hexakis(4′-octyloxybiphenyl-4-yl)-1,4,5,8,9,12-hexaazatriphenylene (6b): glassy yellow solid; mp > 250 °C dec; IR (KBr, cm^{-1}) 2924, 2854, 1605, 1497, 1363, 1247, 822; ^1H NMR ($CDCl_3$) δ 0.90 (t, J = 6.6 Hz, 18 H), 1.30−1.50 (m, 60 H), 1.82 (quint, J = 6.6 Hz, 12 H), 4.00 (t, J = 6.6 Hz, 12 H), 6.97 (d, J = 8.6 Hz, 12 H), 7.60 (d, J = 8.6 Hz, 12 H), 7.62 (d, J = 8.6 Hz, 12 H), 7.96 (d, J = 8.6 Hz, 12 H); MALDI-TOF-MS (positive, dithranol) *m/z* 1916.13 [M^+, calcd for $C_{132}H_{150}N_6O_6$ 1916.16]. Anal. Calcd for $C_{132}H_{150}N_6O_6$: C, 82.72; H, 7.89; N, 4.38. Found: C, 82.64; H, 7.85; N, 4.35.

Data for 2,3,6,7,10,11-hexakis(4′-octylbiphenyl-4-yl)-1,4,5,8,9,-12-hexaazatriphenylene (6c): glassy yellow solid; mp > 250 °C dec; IR (KBr, cm^{-1}) 2923, 2851, 1605, 1496, 1363, 1232, 1192, 1137, 1005, 815; ^1H NMR ($CDCl_3$) δ 0.89 (t, J = 6.4 Hz, 18 H), 1.29−1.66 (m, 72 H), 2.66 (t, J = 6.9 Hz, 12 H), 7.28 (d, J = 8.3 Hz, 12 H), 7.60 (d, J = 8.3 Hz, 12 H), 7.69 (d, J = 8.6 Hz, 12 H), 8.01 (d, J = 8.6 Hz, 12 H); MALDI-TOF-MS (positive, dithranol) *m/z* 1819.57 (M^+, calcd for $C_{132}H_{150}N_6$ 1820.20). Anal. Calcd for $C_{132}H_{150}N_6$: C, 87.08; H, 8.30; N, 4.62. Found: C, 87.11; H, 8.36; N, 4.68.

Data for 2,3,6,7,10,11-hexakis{4′-[(*S*)-3,7-dimethyloctyloxy]-biphenyl-4-yl}-1,4,5,8,9, 12-hexaazatriphenylene (6d): glassy yellow solid; mp > 250 °C dec; IR (KBr, cm^{-1}) 2925, 1605, 1524, 1497, 1364, 1247, 1194, 822; ^1H NMR ($CDCl_3$) δ 0.88 (d, J = 6.6 Hz, 36 H), 0.97 (t, J = 6.4 Hz, 18 H), 1.12−1.90 (m, 80 H), 4.05 (t, J = 6.6 Hz, 12 H), 6.99 (d, J = 8.7 Hz, 12 H), 7.61 (d, J = 8.7 Hz, 12 H), 7.65 (d, J = 8.6 Hz, 12 H), 8.00 (d, J = 8.6 Hz, 12 H);

MALDI-TOF-MS (positive, dithranol) *m*/*z* 2084.94 (M^+, calcd for $C_{144}H_{174}N_6O_6$ 2084.35). Anal. Calcd for $C_{144}H_{174}N_6O_6$: C, 82.95; H, 8.41; N, 4.03. Found: C, 82.79; H, 8.40; N 4.10.

Acknowledgment. We thank Professor Dr. Shigeori Takenaka (Kyushu Institute of Technology) and Dr. Keiichi Otsuka (Kyushu University) for the measurement of MALDI-TOF-MS. This work was partially supported by Supporting Young Researchers with Fixed-term Appointments, Special Coordination Funds for Promoting Science and Technology.

Supporting Information Available: ^{1}H NMR, UV−vis, excitation, and fluorescence spectra, van't Hoff plot for self-association, fluorescence lifetimes, and general experimental procedures. This material is available free of charge via the Internet at http://pubs.acs.org.

JO060768N